17th Australasian Fluid Mechanics Conference
Auckland, New Zealand
5-9 December 2010

A Thermodynamic Model for a High-Pressure Hydrogen Gas Filling System Comprised of Carbon-Fibre Reinforced Composite Pressure Vessels

P.L. Woodfield[1] and M. Monde[2]

[1]Griffith School of Engineering
Griffith University, Gold Coast Campus, Queensland 4215, Australia

[2]Department of Mechanical Engineering
Saga University, Saga 840-8502, Japan

Abstract

Using the geometry of the supply and test vessels and the history of the pressure at the inlet feed line, the model is able to predict the mass flow rate and gas temperature in both the supply and test vessels. The present investigation expands on previous studies [1-4] of the hydrogen vessel filling problem by a simultaneous consideration of the thermal behaviour of supply and test vessels.

Introduction

Hydrogen gas has been proposed as the energy carrier of the future. Ideally, natural or environmentally friendly energy sources will be used to produce hydrogen, for example, via electrolysis of water during periods of low demand for electrical power from consumers. The hydrogen will then be used to power vehicles or to store the energy for later use in other fuel cell applications. In keeping with this vision, hydrogen fuel cell vehicle demonstration projects are currently underway in Japan, Europe and North America. In order to fit the desired 3 to 5 kg of hydrogen onboard a fuel cell passenger vehicle, commercially available carbon-fibre reinforced plastic (CFRP) vessels are being used with pressures from 35 MPa to 70 MPa. The CFRP material is lightweight and very strong but it has a limitation that the temperature is not allowed to exceed 85 °C to conform to current safety legislation. Meeting this requirement is a challenge because it is possible for the gas to approach the limiting temperature during the semi-adiabatic compression process of filling the vessel. Moreover, a lower gas temperature is also desirable to reduce the compression work input and avoid under-filling of the vessel. For public acceptance of the technology the refuelling time is very important and efforts are being made to develop optimized 'fast-filling' systems [1]. Conflicting requirements of a short filling time and lower gas temperatures have been the motivation for thermal experimental investigations on filling of hydrogen vessels [2, 3].

Experiment

A series of experiments were conducted using commercially available CRFP hydrogen pressure vessels for validation of the proposed thermodynamic model for the filling process. As shown in Fig. 1, the supply system consisted of three separate banks of cylinders at different pressures. Filling takes place in a three-stage process to improve the efficiency. The test vessel is partly filled from a low-pressure supply bank (Bank 1) then the supply line is switched to a moderately high pressure supply bank (Bank 2) and then the vessel is finally topped up by the highest pressure supply bank (Bank 3). This procedure is commonly used in demonstration hydrogen filling stations [1]. Note here that Bank 2 in Fig. 1 has the same nominal maximum pressure as Bank 3 but it can be adjusted for the purpose of the experiment. Alternatively, the empty vessel could be filled directly from a single high-pressure source, but more energy would be lost through the non-isentropic throttling process since the pressure drop would be greater on average. The gas temperatures and pressures of the supply banks and test vessel being filled were monitored simultaneously with the environment temperatures and hydrogen gas flow rate. Each vessel consists of an aluminium alloy liner and the load-bearing CFRP material. The liner serves the purpose of sealing the compressed gas and also plays the role of preventing catastrophic failure since the liner is designed to break and release the gas at pressure loads much lower than the upper limit for the reinforced fibre material.

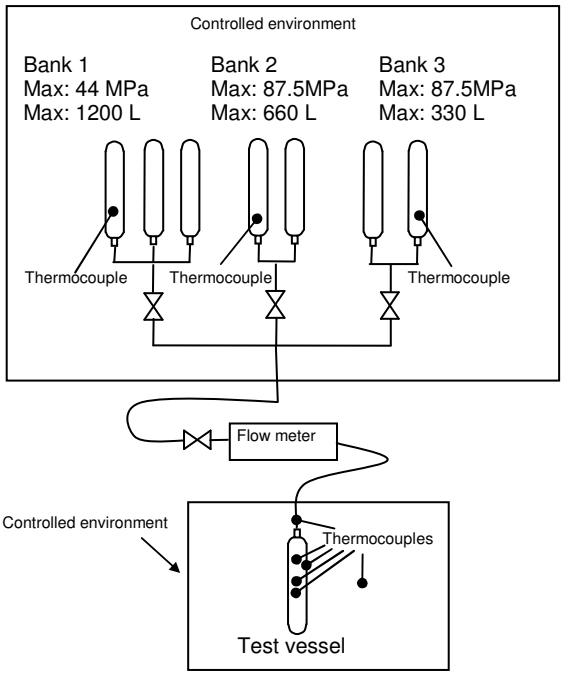

Figure 1. Experimental set up for pressure vessel filling system

Table 1 gives the specifications of the test vessels. The labels 'A' and 'B' represent the two different test vessels considered in this paper. The CFRP material was assumed to have a density of 1530 kg/m^3, a thermal conductivity of 0.55 W/(m·K) and a thermal diffusivity of 0.45×10^{-6} m^2/s. These values correspond to measured properties of CFRP samples from similar pressure vessels analysed in the second author's laboratory.

Test Vessel	A	B
Nominal pressure (MPa)	35	70
Volume (L)	205	130
Inside surface area (m^2)	2.33	1.32
Liner thickness (mm)	4.25	5.25
CFRP thickness (mm)	17	43.5

Table 1. Model input data for test vessels

The thickness of the liners of the supply bank pressure vessels was 4.25 mm. For banks 2 and 3 the CFRP material had a thickness of 34 mm while for bank 1 the thickness was 15.5 mm.

Thermodynamic Model

Figure 2 shows a pictorial representation of the model. At any point in time the test vessel is connected to only one supply bank, thus it is sufficient to model the system shown in Fig. 1 as a transfer of mass and energy between two vessels and heat exchange with the surroundings as shown in Fig. 2. At all times perfectly stirred conditions are assumed for the gas in each vessel. Convection heat transfer to or from the wall is based on the temperature difference between the perfectly stirred gas (i.e. space-averaged gas temperature) and the inside wall surface temperature.

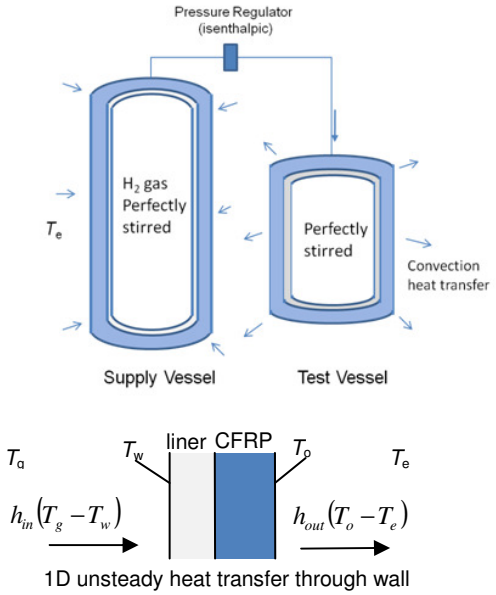

Figure 2. Schematic diagram of thermodynamic model

For either the supply vessel or the test vessel, conservation of energy is represented by an equation in the form of

$$h_{in}A\left(T_w - T_g\right) + \frac{dm}{dt}h_a = \frac{d}{dt}\left(mu\left(P,T_g\right)\right) \tag{1}$$

where m is the mass of hydrogen in the vessel, t is time, T_g is the gas temperature, P is the pressure, u is the specific internal energy, h_a is the specific enthalpy of the gas leaving or entering the vessel, T_w is the inside wall temperature, A is the total inside surface area of the vessel and h_{in} is a convection heat transfer coefficient.

Neglecting the accumulation of mass in the connecting pipeline, mass conservation gives

$$\frac{dm_{\text{supply}}}{dt} = -\frac{dm_{\text{test}}}{dt} \tag{2}$$

Neglecting heat transfer between the flowing gas and the pipe line, and treating the regulator as an isenthalpic device gives

$$h_{\text{supply out}} = h_{\text{test in}} = h_a \tag{3}$$

Note that the supply outlet temperature is lower than the test vessel inlet gas temperature due to the negative Joule-Thomson coefficient and the pressure decrease between the inlet and outlet of the regulator.

Hydrogen is treated as a real gas using data generated by the principle of corresponding states [6]. This data varies within a few percent of the tabulated data for hydrogen gas in Ref. [7] for the pressure and temperature range of interest. Equation (4) is used where the compressibility, Z, is a least-squares polynomial fit to the corresponding states data.

$$\rho\left(P,T_g\right) = \frac{P}{Z\left(P,T_g\right)RT_g} \tag{4}$$

Heat transfer through the wall of the vessel is treated as one-dimensional unsteady heat conduction as in

$$\frac{\partial T_s}{\partial t} = a_s \frac{\partial^2 T_s}{\partial x^2} \tag{5}$$

Where T_s is the temperature of the solid material, a_s is the thermal diffusivity and x is the distance from the inside surface. It is worth mentioning here that including the curvature of the vessel wall in Eq. (5) made only a small difference to the final calculated gas temperatures. The boundary condition for Eq. (5) at the inside wall is given by Eq. (6)

$$-\lambda_s \frac{\partial T_s}{\partial x}\Big|_{x=0} = h_{in}\left(T_g - T_s\,|_{x=0}\right) \tag{6}$$

In Eq. (6) $T_s|_{x=0}$ is the same as T_w in Eq. (1). A similar convection heat transfer boundary condition is specified for the outside of the vessel.

$$-\lambda_s \frac{\partial T_s}{\partial x}\Big|_{x=l} = h_{out}\left(T_s\,|_{x=l} - T_e\right) \tag{7}$$

For the test vessel during charging, the following empirical correlation [4] for the Nusselt number was used to estimate the heat transfer coefficient h_{in}. The characteristic dimension of the vessel D was taken to be the inside diameter of the vessel.

$$\text{Nu}_D = 0.56\,\text{Re}_d^{0.67} + 0.104\text{Ra}_D^{0.352} \tag{8}$$

In Eq. (8) Re_d is the Reynolds number based on the inlet diameter and inlet gas velocity and Ra_D is the Rayleigh number. Transport properties for hydrogen used in Eq. (8) were based on the correlations by Assael et al [8].

During discharging, our previous study [4] suggested that including a term for the forced convection in the relation showed no improvement with respect to correlation of the experimental data than simply using the natural convection relation developed by Daney [5]. Thus for discharging from the supply vessel the following empirical relation [5] was used to determine the inside heat transfer coefficient h_{in}.

$$\text{Nu}_D = 0.104\text{Ra}_D^{0.352} \tag{9}$$

To close the model it is necessary to specify the initial state (pressures and temperatures) and either the mass flow rate into the test vessel or the pressure as a function of time. For the purpose of validating the model we used the measured pressure

history of the test vessel. In our previous study [2] we also used the measured inlet temperature. In the present investigation it is calculated.

Results

Figure 3 shows examples of measured and calculated temperatures in the supply and test vessels. There is a clear correlation between the time for switching the banks (t = 360.5 s; 438 s) and the temperature of the gas in the test vessel. After the vessel has been filled (t = 461 s), the flow stops and the gas cools slowly towards the environment temperature. Conversely the supply banks warm after initially cooling. Generally the agreement is quite good between the model and experimental results (within a few Kelvin for the supply banks and within 10K for the test vessel). The over-estimate of the temperature rise in the test vessel is attributed to the additional heat capacity of the thicker material at the ends of the cylinders and uncertainties in the thermal properties of the CFRP.

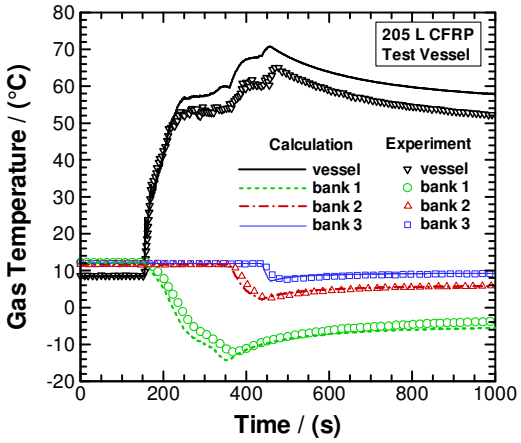

Figure 3. Measured and predicted temperatures of H_2 gas in test vessel 'A' (35 MPa vessel) and supply banks

Figure 4 shows the gas temperature in the supply line. The effect of switching the supply banks is very clear in this figure. Differences between the measured temperature and the model temperature may be attributed to heat exchange between the gas and the pipe and to the time response of the thermocouple. In general the trend is well predicted by the model and may be adequate for hydrogen fuel system design.

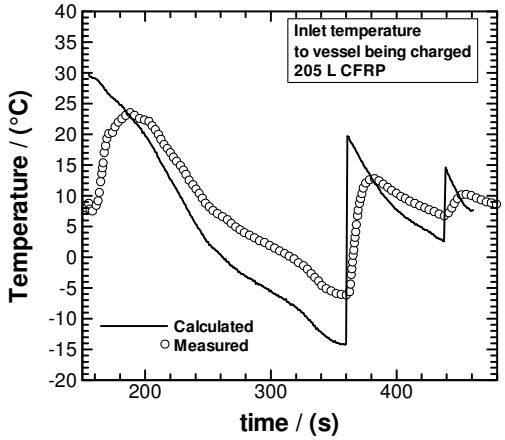

Figure 4. Measured and predicted temperatures in gas line

Figure 5 gives a comparison of the measured and predicted mass of hydrogen in test vessel 'A'. The measured value is integral of the flow meter reading during the experiment. The pressure (dashed line) in Fig. 5 is used as input data for the model. The under prediction of the mass of hydrogen in the vessel corresponds to the over-prediction of the gas temperature shown in Fig. 3 for the test vessel. The mass in the vessel becomes constant after about t = 450 s because the gas flow to the vessel is switched off. The pressure in the vessel decreases slowly after this time while the system is cooling.

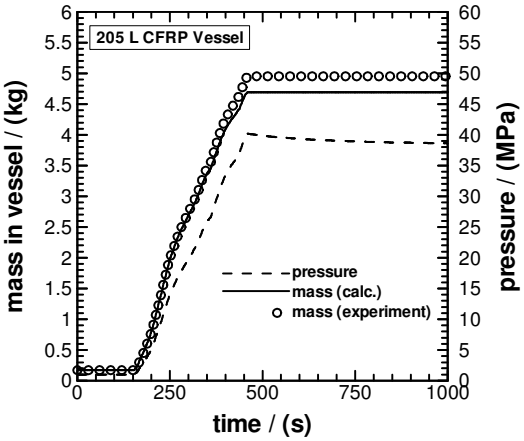

Figure 5. Measured and predicted mass of H_2 gas in test vessel 'A'

Figure 6 gives results for the nominal 70 MPa vessel. For the run shown, the vessel was filled in approximately 10 minutes. The lines show calculated results while the symbols represent experimental temperature data at different positions in the vessel. The dark solid line is the calculated gas temperature. For this case, the predicted temperature is significantly higher (up to 20K) than all of the measured temperatures. This may in part be attributed to effects of the thicker ends of the vessel since the extra heat capacity of these ends is not included in the model. In the lower part of Fig. 6 the calculated outside surface temperature for the vessel is compared with experimental data. The agreement is well within a few K. Although no experimental data are available, calculations of the liner temperature are also shown in Fig. 6. The liner temperature tends to be somewhat lower than the gas temperature. This shows that setting a maximum allowable gas temperature during filling is a conservative restriction since the CFRP material is certainly at a lower temperature.

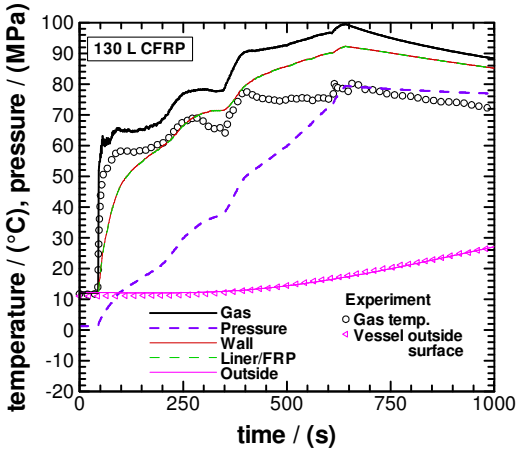

Figure 6. Measured and predicted temperatures of H_2 gas in test vessel 'B' (70 MPa vessel)

Figure 7 shows a comparison of the predicted and measured mass in the nominal 70 MPa pressure vessel for the same test run

shown in Fig. 6. The deviation between the predicted and measured mass of hydrogen is slightly larger in Fig. 7 than for the case shown in Fig. 5. This is consistent with the larger over-prediction of the gas temperature comparing Figs. 6 and 3.

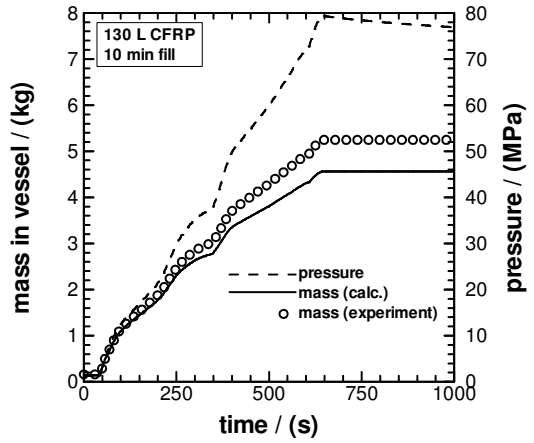

Figure 7. Measured and predicted mass of H_2 gas in test vessel 'B'

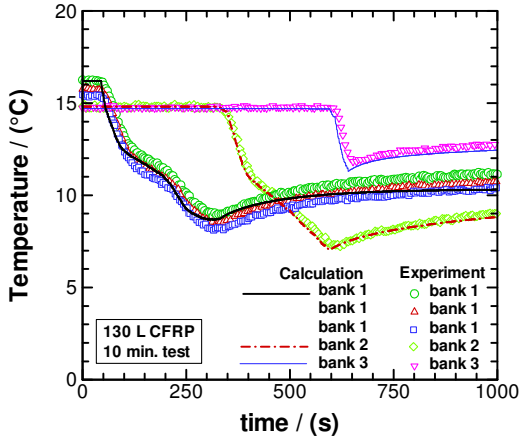

Figure 8. Measured and predicted temperatures in the supply system during filling of vessel 'B' (70 MPa vessel)

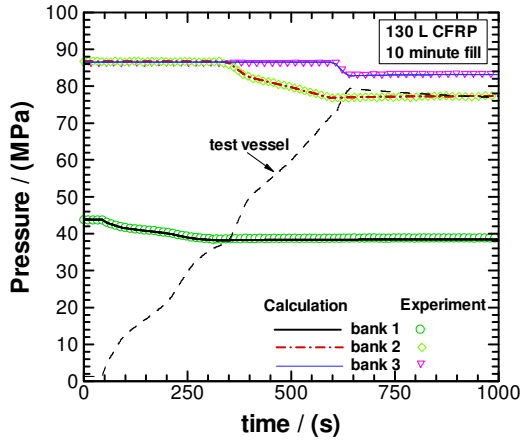

Figure 9. Measured and predicted pressures in the supply system during filling of vessel 'B' (70 MPa vessel)

The predicted temperatures in the supply bank are in good agreement with the measured temperatures for the very high-pressure filling case as shown in Fig. 8. The temperature experimental data for bank 1 are in three different pressure vessels in the bank. The agreement is surprisingly good given the large deviation for the high-pressure test vessel shown in Fig. 6.

Since the model uses only the test vessel pressure as input pressure data, a further point for comparison is the pressures in the supply banks. Figure 9 shows all of the pressures in the system for the case of filling the nominal 70 MPa test vessel. The apparent good agreement in Fig. 9 between experiment and calculation is partly helped by the scale of the figure. Typically there is a deviation of about 0.5 MPa between the experimental result and the calculations in Fig. 9.

Conclusions

In spite of the presence of many simplifications and uncertainties in properties of the CFRP material and uncertainties in heat transfer coefficients, the proposed thermodynamic model successfully approximated the thermal behaviour of a high-pressure hydrogen gas filling system. The largest deviations between model and experiment were for the gas temperature during filling of the nominal 70 MPa vessel. Generally the model over-predicted the gas temperature and consequently under-predicted the mass of hydrogen in the vessel.

References

[1] Zheng, J., Ye, J., Yang, J., Tang, P., Zhao, L., & Kern, M., An Optimized Control Method for a High Utilization Ratio and Fast Filling Speed in Hydrogen Refueling Stations, *Int. J. Hydrogen Energy*, **35**, 2010, 3011-3017.

[2] Woodfield, P.W., Monde, M. & Takano, T., Heat Transfer Characteristics for Practical Hydrogen Vessels being Filled at High Pressure, *J. Thermal Science Tech.*, **3**, 2008, 241-253.

[3] Liu, Y.L., Zhao, Y.Z., Zhao, L., Li, X., Chen, H.G., Zhang., L., Zhao, H., Sheng, R.H., Zie, T., Hu, D.H. & Zheng, J.Y, Experimental Studies on Temperature Rise within a Hydrogen Cylinder During Refueling, *Int. J. Hydrogen Energy*, **35**, 2010, 2627-2632.

[4] Woodfield, P.W., Monde, M. & Mitsutake, Y., Measurements of Averaged Heat Transfer Coefficients in High Pressure Vessel being Charged with Hydrogen, Nitrogen or Argon Gas, *J. Thermal Science Tech.*, **2**, 2007, 180-191.

[5] Daney, D.E., Turbulent Natural Convection of Liquid Deuterium, Hydrogen and Nitrogen within Enclosed Vessels, *Int. J. Heat Mass Transfer*, **19**, 1976, 431-441.

[6] Lee, B.I., Kesler, M.B., A Generalized Thermodynamic Correlation Based on Three-Parameter Corresponding States, *AIChE Journal*, **21**, 1975, 510-527.

[7] Perry, R.H. & Green, D.W., *Perry's Chemical Engineers' Handbook*, 7th Edition, McGraw-Hill, 1997.

[8] Assael, M.J., Mixafendi, S., Wakeham, W.A., The Viscosity and Thermal Conductivity of Normal Hydrogen in the Limit of Zero Density, *J. Phys. Chem. Ref. Data*, 15, 1986, 1315-1322.